Nonalloyed Ohmic Contacts in AlGaN/GaN HEMTs by Ion Implantation With Reduced Activation Annealing Temperature

Felix Recht, L. McCarthy, S. Rajan, A. Chakraborty, C. Poblenz, A. Corrion, J. S. Speck, and U. K. Mishra, *Fellow, IEEE*

***Abstract*—This letter reports AlGaN/GaN high-electron mobility transistors with capless activation annealing of implanted Si for nonalloyed ohmic contacts. Source and drain areas were implanted with an Si dose of 1×10^{16} cm^{-2} and were activated at ~ 1260 °C in a metal–organic chemical vapor deposition system in ammonia and nitrogen at atmospheric pressure. Nonalloyed ohmic contacts to ion-implanted devices showed a contact resistance of 0.96 Ω · mm to the channel. An output power density of 5 W/mm was measured at 4 GHz, with 58% power-added efficiency and a gain of 11.7 dB at a drain bias of 30 V.**

***Index Terms*—Aluminum compounds, gallium compounds, high-electron mobility transistors (HEMTs), ion implantation, modulation-doped field-effect transistors (MODFETs), molecular beam epitaxy (MBE).**

I. Introduction

ION IMPLANTATION is a fundamental manufacturing technique for selective area doping of semiconductor. A number of GaN-based devices processed by ion implantation have been demonstrated [1]–[5]. Previous reports included the use of protective surface layers during the implant activation annealing for devices in the AlGaN/GaN system, including SiO_2 [6], Si_3N_4 [7], and AlN [5], [8]. Yu *et al.* demonstrated ion-implanted AlGaN/GaN high-electron mobility transistors (HEMTs) on sapphire substrates with nonalloyed ohmic contacts. With a reactively sputtered AlN encapsulation layer, the Si activation process employed a high-pressure (100 bar N_2) and high-temperature (~ 1500 °C) annealing process. A contact resistance of 0.4 Ω · mm and an output power of 3.3 W/mm, with a maximum power-added efficiency (PAE) of 54%, were obtained at 4 GHz for a drain bias of 25 V. However, the use of high-temperature high-pressure and capped annealing processes limits the manufacturability of this process for AlGaN/GaN HEMTs. In this letter, we report the use of Si-ion implantation for nonalloyed contacts to an AlGaN/GaN HEMT with a capless implant activation anneal at ~ 1260 °C (thermocouple temperature) in a metal–organic chemical vapor deposition (MOCVD) system. A contact resistance of 0.96 Ω · mm and an output power density of 5 W/mm, with a PAE of 58%, were obtained at 4 GHz for a drain bias of 30 V.

Manuscript received November 30, 2005; revised January 13, 2006. This work was supported in part by grants from the Office of Naval Research, the Center for Advanced Nitride Electronics, and the Defense Advanced Research Projects Agency. The review of this letter was arranged by Editor J. del Alamo.

F. Recht, L. McCarthy, S. Rajan, A. Chakraborty, and U. K. Mishra are with the Electrical and Computer Engineering Department, University of California, Santa Barbara, CA 93106 USA (e-mail: recht@ece.ucsb.edu).

C. Poblenz, A. Corrion, and J. S. Speck are with the Materials Department, University of California, Santa Barbara, CA 93106 USA.

Digital Object Identifier 10.1109/LED.2006.870419

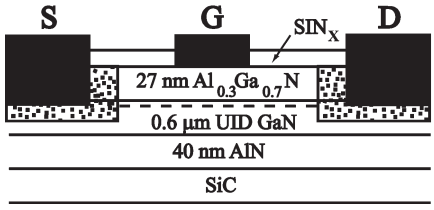

Fig. 1. Schematic epitaxial structure of the implanted AlGaN/GaN HEMT.

II. Device Structure

The HEMT structure described in this letter was grown by RF plasma-assisted molecular beam epitaxy (MBE) on 4H-SiC (0001) (Fig. 1). After a $\sim$ 40-nm AlN nucleation layer, an unintentionally doped (UID) GaN buffer was grown, which was optimized for low buffer leakage current [9]. The buffer was grown with a two-step method to control threading dislocation density [10] and modulated Ga flux for uniformity [11]. The structure had a 27-nm $Al_{0.3}Ga_{0.7}N$ barrier layer. The two-dimensional electron gas sheet density and the Hall mobility, measured using the van der Pauw method at room temperature, were 9.7×10^{12} cm^{-2} and 1640 cm^2/V · s, respectively.

Fabrication of the HEMTs started with the deposition of the ion implantation mask. Fifty nanometers of SiO_2 was deposited by plasma-enhanced chemical vapor deposition (PECVD) at 250 °C. A Ti/Ni mask was evaporated with source and drain (S/D) regions left open for implantation. Subsequently, the SiO_2 layer was removed in the S/D regions using a CF_4 plasma etch. Si ions at a dose of 1×10^{16} cm^{-2} were implanted at 50 keV at room temperature. The sample was tilted 7° relative to the ion source to avoid ion-channeling effects. After the implantation mask was removed, the sample was annealed for activation for 30 s at ~ 1260 °C in an MOCVD system flowing N_2 and NH_3 at atmospheric pressure (760 torr). The AlGaN layer was removed using Cl_2 reactive ion etching (RIE) in the S/D regions, and ohmic Ti/Au/Ni contacts were deposited onto the underlying implanted GaN. Mesa isolation was formed using Cl_2 RIE. The surface was passivated with SiN_x deposited by PECVD. The gate was then deposited using a self-aligned dielectric etch and a metal liftoff process. In order to determine the dominant doping mechanism for the nonalloyed contacts,

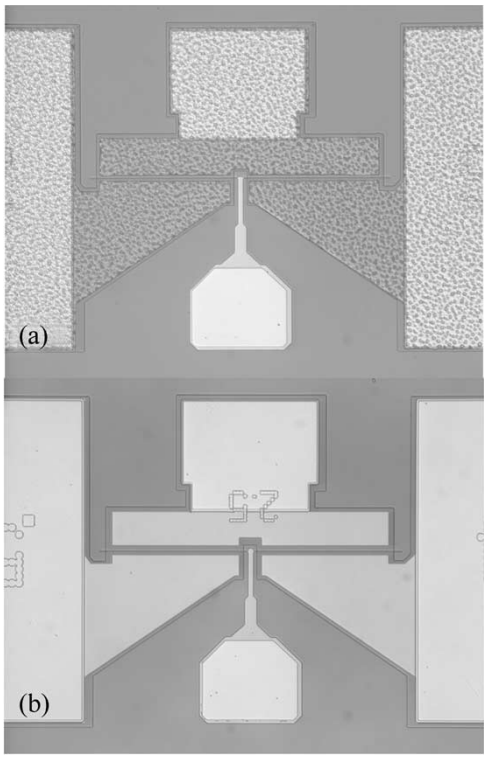

Fig. 2. Optical micrograph of S/D (a) alloyed Ti/Al/Ni/Au and (b) nonalloyed Ti/Au/Ni ohmic contacts and Ni/Au/Ni gate contacts.

additional contacts have been deposited on nonimplanted areas of the implanted sample. Finally, Ti/Au S/D pads were deposited after etching the SiN_x in a CF_4 plasma. A control sample from the same wafer was processed with Ti/Al/Ni/Au contacts alloyed at 870 °C in a rapid-thermal-annealing system but was otherwise processed identically. The gate (width of 2×75 μm) had a length of ~ 0.6 μm for the implanted and ~ 0.5 μm for the control sample. The S/D distance was 3.4 μm.

III. Results and Discussion

Transmission line method (TLM) measurements after passivation showed a contact resistance R_C of 0.96 $\Omega \cdot$ mm and a sheet resistance R_S of 383 Ω/sq for the implanted sample, and an R_C of 0.46 $\Omega \cdot$ mm and an R_S of 344 Ω/sq for the control sample. Simultaneously fabricated contacts on nonimplanted areas of the activation-annealed sample show no ohmic behavior, indicating silicon activation as the dominant mechanism of ohmic contact formation. The nonalloyed contacts showed smooth surface morphology, whereas the alloyed contacts of the control sample showed rough morphology (Fig. 2). The current–voltage output characteristics, dc and under pulsed conditions (200-ns pulsewidth), of the implanted and the control samples are depicted in Fig. 3(a) and (b), respectively. The gate voltage was varied from -4 to $+1$ V in steps of 1 V. The device was biased on a 165-Ω load line. The maximum drain current $I_{\max}$ of the implanted sample was 1.15 A/mm at $V_G = +1$ V, and the pinchoff voltage V_p was -4.4 V. Fig. 3 shows that the 200-ns current values are lower than the dc values, indicating a limited amount of RF-dc dispersion [12]. The control sample showed similar current

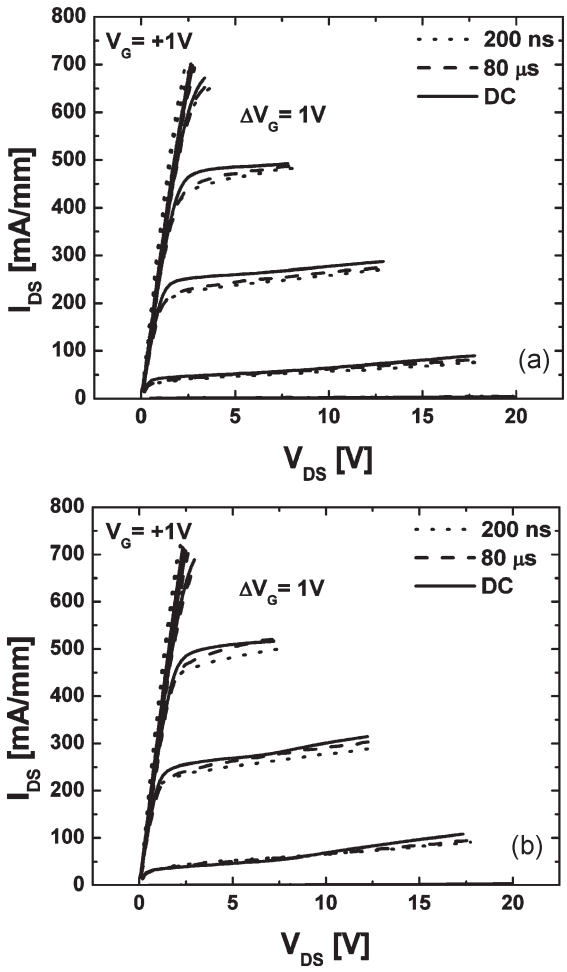

Fig. 3. DC and 200-ns current–voltage curves of (a) implanted and (b) control HEMTs. The gate voltage was varied between -10 and $+1$ V in steps of 1 V, $V_{\mathrm{DSMAX}} = 20$ V. The load line is 165 Ω.

performance, a similar amount of dispersion, $I_{\max} = 1$ A/mm, and $V_p = -5.5$ V. The reduction of $I_{\max}$ and V_p can be attributed to sample inhomogeneity, although further investigation is necessary. Small-signal measurements were carried out on the devices using an Agilent E8361 network analyzer. The current gain h_{21} and the unilateral power gain U were calculated from the measured S-parameters. Linear extrapolation of the current and power gain along a 20-dB/dec slope led to a current maximum gain cutoff frequency f_T of 22 GHz and a maximum oscillation frequency $f_{\max}$ of 49 GHz. The bias conditions were $V_{\mathrm{DS}} = 10$ V and $I_D = 156$ mA/mm. For the control sample, the maximum f_T and $f_{\max}$ were 28 and 65 GHz ($V_{\mathrm{DS}} = 10$ V and $I_D = 189$ mA/mm), respectively.

Finally, power measurements were taken using a Maury Microwave load–pull system. Measurements at 4 GHz and a drain bias of 30 V and a quiescent current of 260 mA/mm showed a gain G_T of 11.7 dB and an output power density P_{out} of 5 W/mm with a PAE of 58% [Fig. 4(a)]. The control device showed comparable power performance with the same P_{out}, a PAE of 49%, and $G_T = 11.7$ dB at $I_D = 260$ mA/mm [Fig. 4(b)]. The slight reduction in PAE is still under investigation, it may be related to the slightly higher gate leakage observed in the control device.

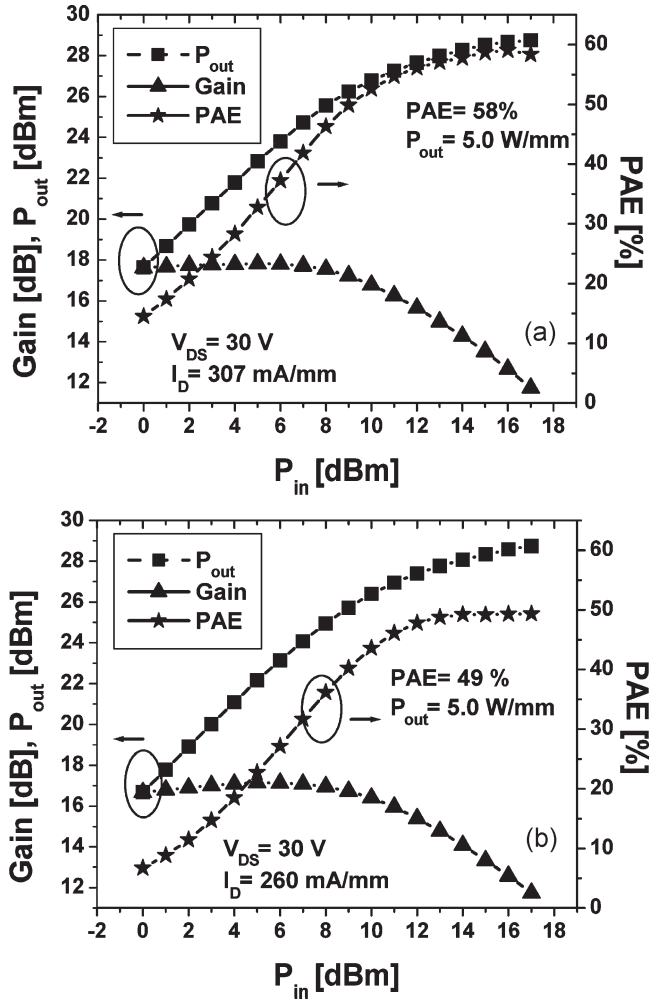

Fig. 4. Load–pull measurements of (a) implanted and (b) control HEMTs at 4 GHz. The device was biased with $V = 30$ V and $I_D = 307$ mA/mm and $I_D = 260$ mA/mm, respectively.

IV. Conclusion

We have demonstrated AlGaN/GaN HEMTs with capless Si-ion implantation activated in an MOCVD system at ~ 1260 °C in N_2 and NH_3 and atmospheric pressure. Nonalloyed ohmic contacts had a contact resistance of 0.96 $\Omega \cdot$ mm to the channel. With a maximum drain current of 1 A/mm, the device showed an f_T of 22 GHz and an $f_{\max}$ of 49 GHz. At 4 GHz, the output power density was 5 W/mm with a PAE of 58% at a drain bias of 30 V. The reduction of implant activation temperature for GaN and the elimination of capping layers enable ion implantation as a practical tool in the processing of GaN-based devices. It has the potential to be utilized in the development of new device topologies as well as in improving the performance and manufacturability of current designs.

Acknowledgment

The authors would like to thank T. Palacios for helpful discussions.

References

[1] J. K. Sheu, M. L. Lee, L. S. Yeh, C. J. Kao, C. J. Tun, M. G. Chen, G. C. Chi, S. J. Chang, Y. K. Su, and C. T. Lee, "Planar GaN n^+-p photodetectors formed by Si implantation into GaN," *Appl. Phys. Lett.*, vol. 81, no. 22, pp. 4263–4265, Nov. 2002.

[2] J. C. Zolper, R. J. Shul, A. G. Baca, R. G. Wilson, S. J. Pearton, and R. A. Stall, "Ion-implanted GaN junction field effect transistor," *Appl. Phys. Lett.*, vol. 86, no. 16, pp. 2273–2275, Apr. 1996.

[3] Y. Irokawa, Y. Nakano, M. Ishiko, T. Kachi, J. Kim, F. Ren, B. P. Gila, A. H. Onstine, C. R. Abernathy, S. J. Pearton, C. C. Pan, G. T. Chen, and J. I. Chyi, "MgO/*p*-GaN enhancement mode metal-oxide semiconductor field-effect transistors," *Appl. Phys. Lett.*, vol. 84, no. 15, pp. 2919–2921, Apr. 2004.

[4] D. Qiao, Z. F. Guan, J. Carlton, S. S. Lau, and G. J. Sullivan, "Low resistance ohmic contacts on AlGaN/GaN structures using implantation and the 'advancing' Al/Ti metallization," *Appl. Phys. Lett.*, vol. 74, no. 18, pp. 2652–2654, May 1999.

[5] H. Yu, L. McCarthy, S. Rajan, S. Keller, S. DenBaars, J. Speck, and U. Mishra, "Ion implanted AlGaN-GaN HEMTs with nonalloyed ohmic contacts," *IEEE Electron Device Lett.*, vol. 26, no. 5, pp. 283–285, May 2005.

[6] Y. Irokawa, O. Fujishima, T. Kachi, S. J. Pearton, and F. Ren, "Activation characteristics of ion-implanted Si^+ in AlGaN," *Appl. Phys. Lett.*, vol. 86, no. 19, pp. 192102-1–192102-3, May 2005.

[7] S. Matsunaga, S. Yoshida, T. Kawaji, and T. Inada, "Silicon implantation in epitaxial GaN layers: Encapsulant annealing and electrical properties," *J. Appl. Phys.*, vol. 95, no. 5, pp. 2461–2466, Mar. 2004.

[8] J. A. Fellows, Y. K. Yeo, R. L. Hengehold, and D. K. Johnstone, "Electrical activation studies of GaN implanted with Si from low to high dose," *Appl. Phys. Lett.*, vol. 80, no. 11, pp. 1930–1932, Mar. 2002.

[9] C. Poblenz, P. Waltereit, S. Rajan, U. K. Mishra, J. S. Speck, P. Chin, I. Smorchkova, and B. Heying, "Effect of AlN nucleation layer growth conditions on buffer leakage in AlGaN/GaN high electron mobility transistors grown by molecular beam epitaxy (MBE)," *J. Vac. Sci. Technol. B, Microelectron. Process. Phenom.*, vol. 23, no. 4, pp. 1562–1567, Jul. 2005.

[10] P. Waltereit, C. Poblenz, S. Rajan, F. Wu, U. K. Mishra, and J. S. Speck, "Structural properties of GaN buffer layers on 4H-SiC(0001) grown by plasma assisted molecular beam epitaxy for high electron mobility transistors," *Jpn. J. Appl. Phys. 2, Lett.*, vol. 43, no. 12A, pp. L1520–L1523, Dec. 2004.

[11] C. Poblenz, P. Waltereit, and J. S. Speck, "Uniformity and control of surface morphology during growth of GaN by molecular beam epitaxy," *J. Vac. Sci. Technol. B, Microelectron. Process. Phenom.*, vol. 23, no. 4, pp. 1379–1385, Jul. 2005.

[12] I. Daumiller, D. Theron, C. Gaquière, A. Vescan, R. Dietrich, A. Wieszt, H. Leier, R. Vetury, U. K. Mishra, I. P. Smorchkova, S. Keller, N. X. Nguyen, C. Nguyen, and E. Kohn, "Current instabilities in GaN-based devices," *IEEE Electron Device Lett.*, vol. 22, no. 2, pp. 62–64, Feb. 2001.